Eigenstructure analysis for the seismic analytical signal in stacking velocity estimation

Tiago Barros (FEEC/UNICAMP) and Renato Lopes (FEEC/UNICAMP)

Abstract

Stacking velocity estimation in seismic processing may be benefit by the use of the complex analytic signal obtained by the Hilbert transform combined with eigenstructure-based methods. In this paper we investigate how the Multiple Signal Classifier is affected by the Hilbert transform. We propose for the complex seismic data a model that approximates the arrival delays as a steering vector for velocities close or equal to the stacking velocity. This approximation helps to interpret the higher-resolution of the eigenstructure-based methods combined with the Hilbert transform. We observed that the eigendecomposition of the complex traces presents a larger concentration of energy in the first eigenimage when compared to the decomposition without the Hilbert transform.

Introduction

Seismic data acquisition is performed in shot-receiver coordinate (Yilmaz, 2001). The recorded data form a common-shot gather with the same shot recorded at different receivers. At each receiver, the recorded data are known as seismic trace. For processing seismic data we can sort the recorded traces in different ways, being one of the most popular the common-midpoint (CMP) method (Mayne, 1962). A CMP gather is formed by putting the traces with the same midpoint between the shot and receiver locations together, with the characteristic that all the traces will be reflections from the same point in depth. In reflection seismic processing, stacking is the operation which uses the diversity property of CMP gathers and generates for each CMP a single zero-offset (ZO) trace. Each sample of the zero-offset trace at time t_0 is generated by summing the amplitudes of the traces in the CMP gather along the normal-moveout (NMO) equation (Dix, 1955), which models the arrival time of reflections in the traces and which depends on the stacking velocity. The process of estimating the stacking velocities in the framework of the CMP method is called velocity analysis (Taner and Koehler, 1969). In this procedure, for each t_0 and each candidate stacking velocity v_k a coherence function is computed. The trial velocity which corresponds to the highest coherence value is chosen as the stacking velocity for that t_0.

The standard coherence function used for velocity analysis is a second-order energy measure called semblance (Neidell and Taner, 1971). In (Biondi and Kostov, 1989) and (Kirlin, 1992), it was shown that coherence measures based on eigenstructure methods, such as the MUltiple SIgnal Classifier (MUSIC) introduced by (Schmidt, 1986), can lead to velocity spectra with higher resolution than semblance. Recently, a seismic MUSIC based on the temporal correlation matrix has been proposed (Barros et al., 2015). On the other hand, the advantages of processing complex analytic seismic traces, obtained by the Hilbert transform, has been discussed since (Taner et al., 1978). In (Sguazzero and Vesnaver, 1986) different coherence measures (some of them using the complex seismic analytical signal) were discussed and it was mentioned in (Biondi and Kostov, 1989) that eigenstructure methods could be benefit by using the complex seismic analytical signal.

Although the use of the Hilbert transform improves the resolution of the velocity stacking estimation, this observation is not explained in the literature. In this paper we discuss and try to explain the impact of the Hilbert transform on the resolution of eigenstructure methods such as MUSIC, as illustrated in (Biondi and Kostov, 1989). In order to do that, we model the arrival delays for the complex seismic data as a steering vector, near the region of the correct stacking velocity. We then analyze the eigendecomposition of the complex seismic traces and present some numerical experiments to support our analysis. Our main observation is that the eigendecomposition of the complex traces presents a larger concentration of energy in the first eigenimage when compared to the decomposition without the Hilbert transform.

Eigenstructure-based coherence

In this section, we first show how the seismic windowed data, which is used by all coherence measures, is formed. Then, we present the spatial and temporal correlation matrices of the windowed data, and show how these matrices yield the MUSIC coherence measures. For further detail, we encourage the reader to see (Barros et al., 2015).

Windowed data

Coherence is computed on a window of data centered at some time $\tau_k(i)$, where k corresponds to a given value of the velocity being tested and i denotes a trace. Consider the windowed data with N_t samples formed by $L = (N_t - 1)/2$ samples above and below the NMO traveltime, defined by the zero-offset traveltime t_0 and a trial velocity v_k as

$$\tau_k(i)^2 = t_0^2 + \frac{4h_i^2}{v_k^2}, \tag{1}$$

where h_i is the half-offset between the source and receiver that generated the trace. When a window is formed with the correct value of v_k, in a t_0 that contains a seismic event, the seismic signal in all the traces will contain a reflection, and thus the samples in the traces will be highly correlated. In that case a coherence function computed from the windowed data will present a large value, indicating that the velocity v_k yields a good fit.

Remember that N_t is the number of samples in the window and let N_r be the number of traces in the CMP gather. For each t_0, we can model the seismic windowed data as (Barros et al., 2015)

$$\mathbf{D} = \mathbf{1}\mathbf{s}^T + \mathbf{N}, \tag{2}$$

where the dimension of $\mathbf{D}$ is $N_r \times N_t$, $\mathbf{s}$ is the seismic *wavelet* with dimension $N_t \times 1$, $\mathbf{1}$ is a vector of all-ones with dimension $N_r \times 1$ and $\mathbf{N}$ is an $N_r \times N_t$ error matrix. In the sequel, we briefly review how this model yields the MUSIC coherence measure.

Multiple signal classification

The windowed spatial correlation matrix can be written as

$$\mathbf{R} = \frac{1}{N_t}\mathbf{D}\mathbf{D}^T \approx \frac{||\mathbf{s}||^2}{N_t}\mathbf{1}\mathbf{1}^T + \sigma_n^2\mathbf{I}, \tag{3}$$

where $||\mathbf{s}||^2$ is the energy of the wavelet, σ_n^2 is the noise variance and $\mathbf{I}$ is the identity matrix of appropriate dimension. The matrix $\mathbf{R}$ is called *spatial* correlation matrix because it measures the correlation between different traces, i.e., different spatial coordinates. Its dimension is $N_r \times N_r$. If there is an event in the window, $\mathbf{1}$ is approximately an eigenvector of $\mathbf{R}$ associated with its largest eigenvalue. In this paper, we will refer to this as the largest eigenvector of $\mathbf{R}$. In the literature, MUSIC methods are based on the sample spatial correlation matrix $\mathbf{R}$, so they will be called spatial, or S-MUSIC (Wang et al., 2001). Essentially, they can be seen as an attempt to answer the question: “Is the all-ones vector $\mathbf{1}$ proportional to the largest eigenvector or $\mathbf{R}$?” If this answer is positive, then we may assume that $\mathbf{R}$ was formed from a window that contains a reflection. The S-MUSIC coherence measure is given by

$$P_S = \frac{N_r}{N_r - |\mathbf{1}^T\mathbf{v}_1|^2}, \tag{4}$$

where $\mathbf{v}_1$ is the largest eigenvector of $\mathbf{R}$, with dimension $N_r \times 1$. If the window is well-matched to a single event, then P_S will be infinity.

As with the spatial correlation, the temporal correlation matrix can be computed from the data as

$$\mathbf{r} = \frac{1}{N_r}\mathbf{D}^T\mathbf{D} \approx \mathbf{s}\mathbf{s}^T + \sigma^2\mathbf{I}. \tag{5}$$

In this equation, σ^2 is the noise variance for the temporal correlation matrix, which is not necessarily equal to σ_n^2 from the spatial correlation matrix. The dimension of the matrix $\mathbf{r}$ is $N_t \times N_t$. The matrix $\mathbf{r}$ contains the correlation between different time samples of the windowed data, and is thus called a *temporal* correlation matrix. The corresponding coherence measure is called T-MUSIC.

It can be shown that if there is an event in the window, the largest eigenvalue of $\mathbf{r}$ is $\lambda_1 \approx ||\mathbf{s}||^2 + \sigma^2$, associated with the eigenvector $\mathbf{u}_1 \approx \mathbf{s}$. Therefore, instead of testing whether the all-ones vector, $\mathbf{1}$, is the largest eigenvector of $\mathbf{R}$, as is done in S-MUSIC, we may test whether $\mathbf{s}$ is the largest eigenvector of $\mathbf{r}$. To compute a coherence measure from $\mathbf{r}$ without knowledge of $\mathbf{s}$, we use the fact that the eigenstructures of $\mathbf{R}$ and $\mathbf{r}$ are related. It can also be shown that if $\mathbf{1}$ is the largest eigenvector of $\mathbf{R}$, we expect that $\mathbf{D}^T\mathbf{1}$ is the largest eigenvector of $\mathbf{r}$. The term $\mathbf{D}^T\mathbf{1}$ has an interesting interpretation. Indeed, let

$$\hat{\mathbf{s}} = \frac{1}{N_r}\mathbf{D}^T\mathbf{1}. \tag{6}$$

Now, recall that, if t_0 and v_k are correct, then all the traces in the window contain repetitions of the seismic wavelet $\mathbf{s}$. Also note that $\hat{\mathbf{s}}$ is the mean value of the traces in a window, and can thus be seen as an estimate of the wavelet $\mathbf{s}$. In consequence, we see that T-MUSIC tries to answer the question “Is the largest eigenvector of $\mathbf{r}$ proportional to the estimated wavelet?” The resulting T-MUSIC coherence measure is given by

$$P_T = \frac{||\hat{\mathbf{s}}||^2}{||\hat{\mathbf{s}}||^2 - |\hat{\mathbf{s}}^T\mathbf{u}_1|^2}, \tag{7}$$

where $\mathbf{u}_1$ is the largest eigenvector of $\mathbf{r}$, with dimension $N_t \times 1$. If $\hat{\mathbf{s}}$ is the largest eigenvector of $\mathbf{r}$, then P_T will be infinity.

Complex analytical trace

As defined in (Taner et al., 1978) complex seismic trace analysis treats seismic traces as the real part of analytical complex traces. The analytical seismic trace can be computed as:

$$x(t) = d(t) + j\mathscr{H}\{d(t)\}, \tag{8}$$

where $\mathscr{H}\{d(t)\}$ is the Hilbert transform of the seismic signal $d(t)$.

Let $D(f)$ be the continuous-time Fourier transform of $d(t)$, then the analytical signal can be defined in frequency domain as

$$X(f) = \begin{cases} 2D(f), & \text{if} \quad f \geq 0 \\ 0, & \text{if} \quad f < 0 \end{cases}. \tag{9}$$

Thus, the analytical signal is a complex-valued signal with only positives frequencies, but its frequencies amplitudes have twice the value of the ones from the real-valued seismic signal.

The windowed analytical seismic data can then be written as

$$\mathbf{X}^T = \mathbf{D}^T + j\mathbf{H}\mathbf{D}^T, \tag{10}$$

where superscript T denotes transpose operation. The matrix $\mathbf{H}$ is an $N_t \times N_t$ convolution matrix that contains the coefficients of the Hilbert transform:

$$\mathbf{H} = \begin{bmatrix} \mathbf{h}_1 \\ \vdots \\ \mathbf{h}_{N_t} \end{bmatrix}. \tag{11}$$

Each row of $\mathbf{H}$ is a $1 \times N_t$ vector with the coefficients that generate the corresponding row of the Hilbert transform for each column of $\mathbf{D}^T$. We can also write $\mathbf{X}^T$ as

$$\mathbf{X}^T = \tilde{\mathbf{H}}\mathbf{D}^T, \tag{12}$$

where $\tilde{\mathbf{H}} = \mathbf{I} + j\mathbf{H}$. This matrix notation will be useful to the development of the next sections.

Steering vector approximation for the analytical signal

In this section we propose a steering vector approximation to the complex seismic windowed data. This approximation helps to interpret the eigenstructure of seismic analytical signal when the velocity used to form the window is close or equal to the velocity of the seismic event. In these cases the reflections events will not be aligned in the window. The events will arrive with a small delay along the traces, which might be modeled as a steering vector.

First, let $d_1(t)$ be the continuous-time signal whose samples form the data for the first trace in the window. In other words, the first row of $\mathbf{D}$ consists of the vector

$$\mathbf{d}_1 = [d_1(dt) \cdots d_1(N_t\, dt)], \tag{13}$$

with dimension $1 \times N_t$, being dt the sample period. Now, assume that the signal at each trace is a delayed version of the signal at the first receiver. In other words, the continuous-time signal for the i-th trace is $d_i(t) = d(t-\theta_i)$, where θ_i is the delay. Now, if we assume that the delay θ_i is sufficiently small when compared to the bandwidth of the signals, we may use the *narrowband* approximation and write:

$$x_i(t) = x_1(t-\theta_i) \approx x_1(t)e^{j\theta_i}, \tag{14}$$

where $x_i(t)$ is the Hilbert transform of $d_i(t)$.

With this approximation in mind, we may write the analytical seismic windowed data as

$$\mathbf{X}^T = \mathbf{x}_1^T \mathbf{a}^T + \mathbf{N}, \tag{15}$$

where $\mathbf{x}_1$ is a $1 \times N_t$ vector with the analytical signal at the first receiver

$$\mathbf{x}_1 = [x_1(dt) \cdots x_1(N_t\, dt)] \tag{16}$$

and $\mathbf{a}$ is an $N_r \times 1$ steering vector with the delays for each receiver

$$\mathbf{a}^T = [1\, e^{j\theta_1} \cdots e^{j\theta_{N_r-1}}]. \tag{17}$$

MUSIC for the analytical signal

The MUSIC coherence functions can be computed from the analytical signal, as indicated in (Biondi and Kostov, 1989). If we use the analytical signal from equation (15) we would have spatial and temporal correlation matrices defined by equations (18) and (19):

$$\mathbf{R}_X = \frac{1}{N_t}\mathbf{X}\mathbf{X}^H \approx \frac{1}{N_t}||\mathbf{x}_1||^2\mathbf{a}\mathbf{a}^H + \sigma_n^2\mathbf{I}. \tag{18}$$

$$\mathbf{r}_X = \frac{1}{N_r}\mathbf{X}^H\mathbf{X} \approx \mathbf{x}_1^H\mathbf{x}_1 + \sigma^2\mathbf{I}. \tag{19}$$

The superscript H denotes hermitian operation. It can be shown that the largest eigenvectors from $\mathbf{R}_X$ and $\mathbf{r}_X$ are approximately $\mathbf{a}$ and $\mathbf{x}_1$, respectively. We can compute MUSIC coherence functions using equations (4) and (7), replacing the eigenvectors $\mathbf{v_1}$ and $\mathbf{u_1}$ by the largest eigenvectors from $\mathbf{R}_X$ and $\mathbf{r}_X$, respectively.

The steering vector approximation is good for small delays and is exact if the seismic signal is aligned in the window. If that is the case, we have $\mathbf{a} = \mathbf{1}$ (the delays are all equal to zero) and in ideal conditions, the signal at the first receiver will be the seismic *wavelet* $\mathbf{s}$. So, the largest eigenvector from $\mathbf{R}_X$ will be close to $\mathbf{1}$ and the largest eigenvector from $\mathbf{r}_X$ will be close to the analytical version of the largest eigenvector from $\mathbf{r}$ ($\mathbf{x}_1 \approx \tilde{\mathbf{H}}\mathbf{s}^T$). We analyze in section the cases where the window is a close but imperfect fit to the data.

Numerical results

Synthetic data

In order to compare the MUSIC coherence function with and without the analytical signal, we first used a simple synthetic model with a single reflection. We generated this data using equation (1), with a zero-offset traveltime of $1\,$s and a velocity of $2100\,$m/s. The reflection was modeled by a zero-phase Ricker wavelet (Hosken, 1988), with a dominant frequency of $20\,$Hz. The CMP section contains 101 traces. The offset of the first one is $80\,$m and the distance between them is $40\,$m. The sample period is $2\,$ms. We also added Gaussian noise to the data, in order to get the average signal-to-noise ratio (SNR) of approximately $15\,$dB along the event.

In $t_0 = 1\,$s, we computed both S- and T-MUSIC for several trial velocities. The results are shown in Fig. 1, where can be seen that in both cases the MUSIC computed with the analytical signal present a better resolution. We explain this by the fact that in windows formed with velocities that are close to the actual velocity the eigenvectors from $\mathbf{R}_X$ and $\mathbf{r}_X$ are not close to $\mathbf{1}$ and $\mathbf{s}$, as discussed in section . Their projections onto $\mathbf{1}$ and $\mathbf{s}$ do not result in values close to zero in the denominator of equations (4) and (7). So, the values of P_S and P_T will be smaller than the values obtained without the analytical signal, as illustrated in Fig. 1.

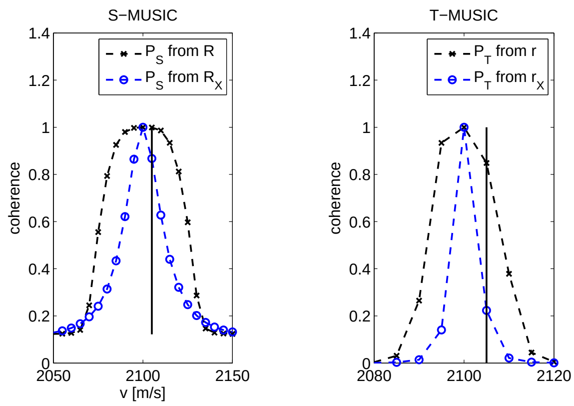

(a) (b)

Figure 1: S-MUSIC (a) and T-MUSIC (b) plot for the example. The vertical lines are placed in $v = 2105\,$m/s to illustrate the difference when using the analytical signal.

In Fig. 1, we draw a vertical line at $v = 2105\,$m/s, which is a velocity close to the stacking velocity where there is a difference in the coherence computed with and without the analytical signal. This difference might be explained by the steering vector approximation. The largest eigenvectors of $\mathbf{R}_X$ and $\mathbf{r}_X$ represent events that are not exactly aligned, arriving with small delays along the traces. So they are more different of $\mathbf{1}$ and $\mathbf{s}$ than the largest eigenvectors from $\mathbf{R}$ and $\mathbf{r}$, which results in this gain of resolution.

In Fig. 2 and Fig. 3 we show the frequency spectra from the eight largest eigenvectors from $\mathbf{r}$ and $\mathbf{r}_X$ at $v = 2105\,\mathrm{m/s}$. (The frequency axis are in normalized frequencies going from 0 to 2π.) For a better visualization of the eigenvectors we did not added Gaussian noise to generate Fig. 2 and Fig. 3. It is possible to see that the positives frequencies from eigenvectors 1 and 2 of $\mathbf{r}$ are similar to the positive frequencies of the eigenvector 1 from $\mathbf{r}_X$. This observation also holds for other eigenvectors in the figures. This is an indication that the energy in the eigendecomposition of $\mathbf{r}$ corresponding to two distinct eigenvectors may be concentrated in a single eigenvector of $\mathbf{r}_X$.

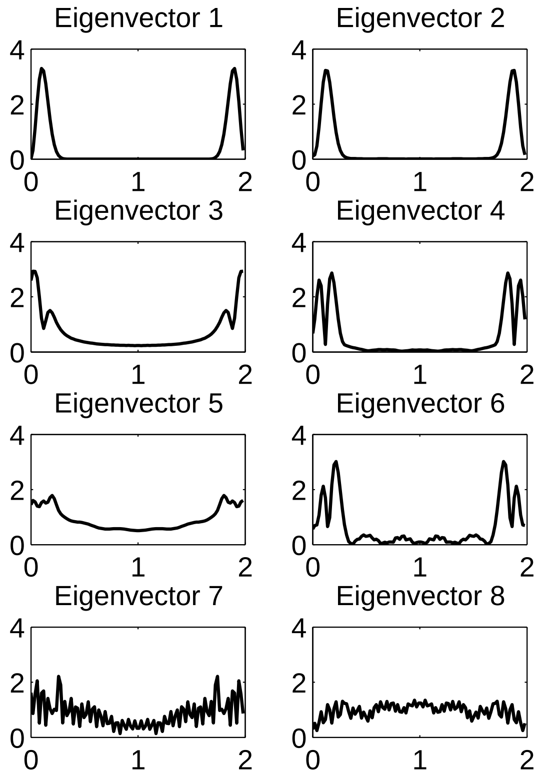

Figure 2: Frequency spectra from the eight largest eigenvectors from $\mathbf{r}$.

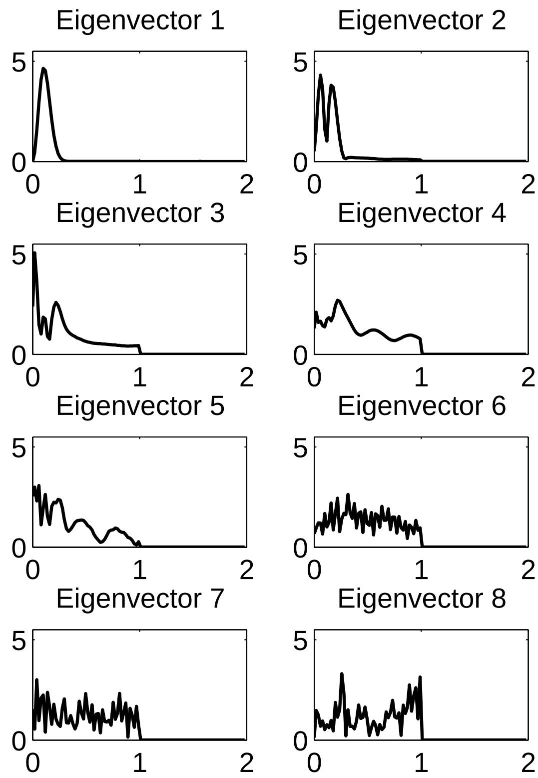

Figure 3: Frequency spectra from the eight largest eigenvectors from $\mathbf{r}_X$.

In Fig. 4 we show for the range of velocities between $1000\,\mathrm{m/s}$ and $3000\,\mathrm{m/s}$ the largest eigenvalue from $\mathbf{r}$, λ_1, compared with the largest eigenvalue from $\mathbf{r}_X$, λ_{1H}. We also show in Fig. 4 the sum of the two largest eigenvalues from $\mathbf{r}$, $\lambda_1 + \lambda_2$, compared with λ_{1H}. It is possible to see that $\lambda_1 + \lambda_2$ are very close to λ_{1H}, which is also a indication that the energy in two eigenvectors of $\mathbf{r}$ is concentrated in a single eigenvector of $\mathbf{r}_X$.

Field data

We tested the computation of MUSIC coherence function with and without the analytical signal in a marine field data set, acquired in the Jequitinhonha Basin and provided by PETROBRAS. The data set contains 981 shots with a distance of $25\,\mathrm{m}$ between consecutive shots. There are 120 receivers displaced with intervals of $25\,\mathrm{m}$ for each shot. The sample period is $4\,\mathrm{ms}$ and the total recording time is $7\,\mathrm{s}$.

In Fig. 5 we show the CMP from the marine field data which we used in the tests and the velocity spectrum computed with semblance. We show the velocity spectra computed with and without the analytical signal for S-MUSIC, in Fig. 6, and T-MUSIC, in Fig. 7. In this field data it is not possible to distinguish an improvement in the resolution, with the use of the analytical signal. However, in Fig. 7 we indicate with red arrows a small region where the use of the analytical signal presents an interesting difference: the velocity of the event indicated is smaller when the T-MUSIC is computed with the analytical signal. Possibly, when we used the analytical signal we corrected the small deviations in phase and the event was properly fitted in the window. This event might also be a repetition of the above event fitted in the window, once they are close in time and its velocities are approximately the same.

Conclusions

In this paper we discuss the use of the seismic analytic signal for eigenstructure-based stacking velocity estimation. We observe that the analytical signal increases the resolution of MUSIC coherence function and propose a steering vector approximation to be used in the velocity search when we have velocities close or equal to the stacking velocity. This approximation explains the higher-resolution of MUSIC for the analytical signal and showed

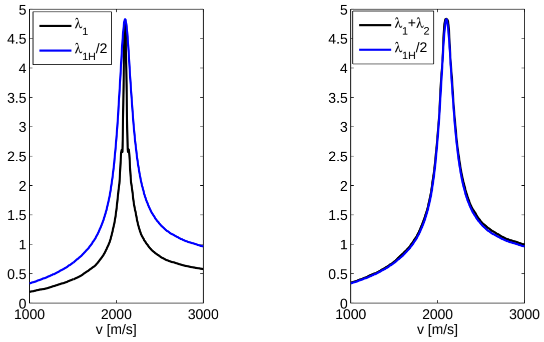

(a) (b)

Figure 4: Comparison of eigenvalues from $\mathbf{r}$ and $\mathbf{r}_X$: (a) The black line is the largest eigenvalue from $\mathbf{r}$, λ_1, and the blue line is the largest eigenvalue from $\mathbf{r}_X$, λ_{1H}; (b) The black line is the sum of the two largest eigenvalues from $\mathbf{r}$, $\lambda_1 + \lambda_2$, and the blue line is the largest eigenvalue from $\mathbf{r}_X$, λ_{1H}.

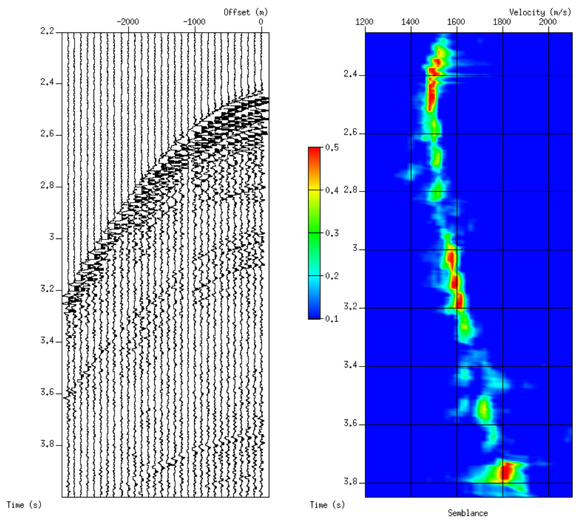

(a) (b)

Figure 5: CMP section (a) and its semblance coherence panel (b) .

to be valid in synthetic numerical experiments. We also observe, in synthetic numerical experiments, that the eigendecomposition of the seismic analytical signal seems to concentrate the energy in the largest half of the eigenvalues when compared to the eigendecomposition of the real-valued seismic signal. We compare for a marine field data the velocity spectra computed with and without the analytical signal. For the marine field data, we do not observe an improvement in the resolution with the use of the analytical signal, but we observe an indication that the analytical signal might be useful to estimate velocities with more precision. For a better understanding of the benefits of the analytical signal in the computation of eigenstructure-based velocity spectra, more tests with real seismic data must be made.

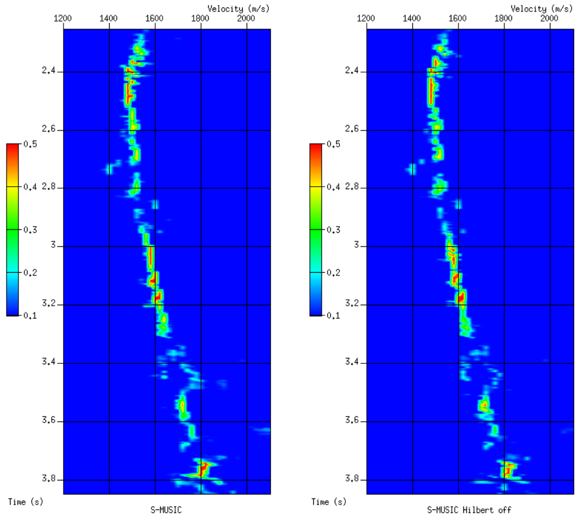

(a) (b)

Figure 6: S-MUSIC coherence panel computed with (a) and without (b) the analytical signal.

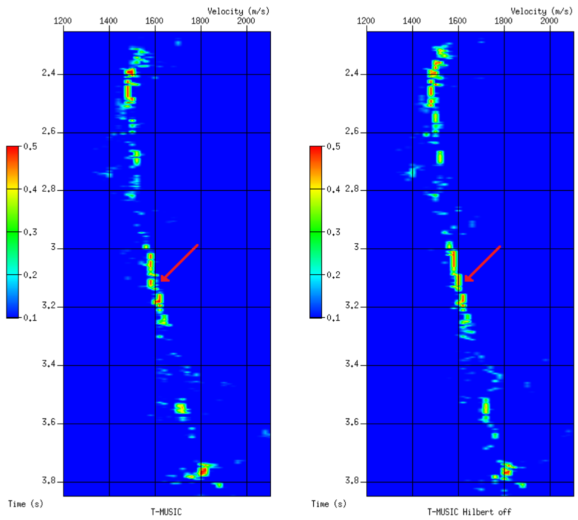

(a) (b)

Figure 7: T-MUSIC coherence panel computed with (a) and without (b) the analytical signal.

Acknowdegments

The authors thank CNPq, INCT-GP/CNPQ (www.inct-gp.org) and PETROBRAS for the financial support.

References

Barros, T., R. Lopes, and M. Tygel, 2015, Implementation aspects of eigendecomposition-based high-resolution velocity spectra: Geophysical Prospecting, **63**, 99–115.

Biondi, B., and C. Kostov, 1989, High-resolution velocity spectra using eigenstructure methods: Geophysics, **54**, 832–842.

Dix, C. H., 1955, Seismic velocities from surface measurements: Geophysics, **20**, 68–86.

Hosken, J., 1988, Ricker wavelets in their various guises: First Break, **6**.

Kirlin, R. L., 1992, The relationship between semblance and eigenstructure velocity estimators: Geophysics, **57**, 1027–1033.

Mayne, W. H., 1962, Common reflection point horizontal data stacking techniques: Geophysics, **27**, 927–938.

Neidell, N., and M. Taner, 1971, Semblance and other coherency measures for multichannel data: Geophysics, **36**, 482–497.

Schmidt, R. O., 1986, Multiple emitter location and signal parameter estimation: IEEE Transactions on Antennas and Propagation, **34**, 276–280.

Sguazzero, P., and A. Vesnaver, 1986, A comparative analysis of algorithms for stacking velocity estimation: Bernabini M., Carrin P., Jacovitti G., Rocca F., Treitel S., Worthington MH, Ed, 267–286.

Taner, M., and F. Koehler, 1969, Velocity spectra digital computer derivation and applications of velocity functions: Geophysics, **34**, 859–881.

Taner, M., F. Koehler, and R. Sheriff, 1978, Complex seismic trace analysis: Geophysics, **44**, 1041–1063.

Wang, Y., J. Chen, and W. Fang, 2001, TST-MUSIC for joint DOA-delay estimation: IEEE Transactions on Signal Processing, **49**, 721–729.

Yilmaz, O., 2001, Seismic data analysis: Processing, inversion, and interpretation of seismic data, volume 1, 2nd ed.: Society of Exploration Geophysicists.